APOC1 promotes the progression of osteosarcoma by binding to MTCH2

RENJIE LI[1], HUIXIAN HE[2] and XINXIN HE[3]

[1]School of Nursing, Sun Yat-Sen University; [2]Department of Gastroenterology and Hepatology, The First Affiliated Hospital of Sun Yat-Sen University, Guangzhou, Guangdong 510080; [3]School of Medicine, Foshan University, Foshan, Guangdong 528000, P.R. China

Received April 8, 2022; Accepted January 6, 2023

DOI: 10.3892/etm.2023.11862

Abstract. Osteosarcoma is the most prevalent primary malignant bone cancer worldwide. Apolipoprotein C1 (APOC1) and mitochondrial carrier homolog 2 (MTCH2) have been identified to be upregulated during the oncogenesis and metastasis of osteosarcoma. The aim of the present study was to explore the role of APOC1 in osteosarcoma progression and the mechanisms associated with MTCH2. APOC1 and MTCH2 expression in osteosarcoma cells was assessed by reverse transcription-quantitative PCR and western blotting. Then, APOC1 was silenced to detect its effect on cell viability, proliferation and apoptosis using Cell Counting Kit-8, a colony formation assay and TUNEL staining, respectively. Transwell and wound healing assays were used to evaluate cell invasion and migration. The interaction between APOC1 and MTCH2 as predicted by the Biological General Repository for Interaction Datasets and the Search Tool for the Retrieval of Interacting Genes/Proteins databases was verified by co-immunoprecipitation assay. Subsequently, rescue experiments were performed to analyze the regulatory effects of APOC1 on MTCH2 in the biological behavior and Warburg effect of osteosarcoma cells. Significantly upregulated APOC1 and MTCH2 expression was found in osteosarcoma SAOS-2 cells. APOC1 silencing attenuated cell viability, inhibited proliferation and promoted cell apoptosis, coupled with the decreased Bcl-2 expression and increased Bax and cleaved-caspase 3 expression. The invasive and migratory capacities of SAOS-2 cells were also suppressed following APOC1 knockdown. Moreover, APOC1 was confirmed to interact with MTCH2 in osteosarcoma cells. MTCH2 upregulation inhibited the impacts of APOC1 deletion on the malignant behavior of osteosarcoma cells. APOC1 silencing-induced oxidative phosphorylation elevation and Warburg effect decrease were partially restored by MTCH2 upregulation. In sum, APOC1 promoted progression of osteosarcoma by binding to MTCH2, suggesting that targeting the APOC1/MTCH2 axis may be a potential treatment of osteosarcoma.

Correspondence to: Dr Xinxin He, School of Medicine, Foshan University, 5 Hebin Road, Chancheng, Foshan, Guangdong 528000, P.R. China
E-mail: xinxinhesunshine@163.com

Key words: osteosarcoma, apolipoprotein C1, mitochondrial carrier homolog 2, invasion, Warburg effect

Introduction

Osteosarcoma is the most prevalent primary malignant bone cancer worldwide, characterized by early lung metastasis and poor prognosis, which poses threats to adolescents and young adults (coinciding with rapid bone growth) due to complications and distal metastasis (1,2). Despite progress in modern treatment for osteosarcoma, including chemotherapy, surgery, neoadjuvant therapy and combination therapy, the cure rate is poor and the 5-year survival rate of patients with osteosarcoma remains <30% due to the highly aggressive behaviors of osteosarcoma cells and propensity to metastasize (3,4). Therefore, it is imperative to uncover the molecular mechanisms responsible for osteosarcoma occurrence to discover a novel and effective target for therapeutic intervention.

Apolipoprotein C1 (APOC1), located at 19q13.32, is a member of the apolipoprotein C family. As a component of triglyceride-rich and high-density lipoproteins, APOC1 serves a significant role in lipid transport and metabolism (5,6). The key role of APOC1 in the occurrence and development of numerous cancers has been highlighted by an increasing number of studies (7-9). For example, APOC1 has been reported as a novel prognostic biomarker in colorectal cancer for its inhibitory effects on progression of colorectal cancer (7). Shi *et al* (8) demonstrated the pro-carcinogenic effects of APOC1 in the pathogenesis of cervical cancer. By suppressing cell proliferation, migration and invasion, APOC1 silencing has an inhibitory effect on the progression of esophageal cancer (9). APOC1 expression is continuously upregulated in osteosarcoma tissue samples during the occurrence and metastasis of osteosarcoma, as demonstrated by the analysis of gene expression profiles (10). However, the specific effects of APOC1 on the development of osteosarcoma remain to be elucidated.

As an important regulator of mitochondrial metabolism and cell death, MTCH2 expression is upregulated in clinical osteosarcoma samples (11,12). MTCH2 is a suppressor of oxidative phosphorylation (OXPHOS), and the metabolic switch from OXPHOS to glycolysis is a hallmark of osteosarcoma (13,14).

Under aerobic conditions, most normal differentiated cells generate energy by mitochondrial OXPHOS (15). By contrast, most cancer cells undergo glycolysis even in the presence of sufficient oxygen, which stimulates tumor cells to gain sufficient energy for proliferation and distant metastasis; this phenomenon was first reported by Otto Warburg and is known as the Warburg effect (16-18). Upregulation of OXPHOS and inhibition of glycolysis can restrain proliferation of osteosarcoma cells (19). Therefore, it was hypothesized that APOC1 could interact with MTCH2 to promote the Warburg effect and malignant development of osteosarcoma cells.

In the present study, the effects of APOC1 on the proliferation, apoptosis, invasion and migration of osteosarcoma cells were investigated. Whether APOC1 affects the progression of osteosarcoma by binding to MTCH2 was also investigated. The present study aimed to provide new insights into the pathogenesis of osteosarcoma and identify novel targets for the treatment of this disease.

Materials and methods

Bioinformatics tools. The Biological General Repository for Interaction Datasets (BioGRID) (20) and Search Tool for the Retrieval of Interacting Genes/Proteins (STRING) databases (21) were employed to predict the interaction between APOC1 and MTCH2.

Cell culture. Human osteosarcoma (HOS, SAOS-2, 143B and U2OS) and the human osteoblast cell line hFOB1.19 were obtained from the Type Culture Collection of the Chinese Academy of Sciences. HOS, SAOS-2, 143B and U2OS cells were cultured using RPMI-1640 medium (HyClone; Cytiva) and hFOB1.19 cells were cultivated in DMEM (HyClone; Cytiva) in a humid atmosphere with 5% CO_2 at 37˚C. All media were mixed with 10% fetal bovine serum (FBS; Gibco; Thermo Fisher Scientific, Inc.).

Cell transfection. For transfection, short hairpin RNAs (shRNAs) targeting APOC1 (sh-APOC1-1, 5'-TTCAGAAAG TGAAGGAGAAAC-3' and sh-APOC1-2, 5'-GTCTCCAGT GCCTTGGATAAG-3'), corresponding negative control (sh-NC, 5'-UUCUCCGAACGUGUCACGUTT-3'), MTCH2 pcDNA3.1 plasmid (Oe-MTCH2; cat. no. NM_001317231.2) and the empty vector control (Oe-NC) were supplied by Guangzhou RiboBio Co., Ltd. SAOS-2 cells were cultured in 6-well plates to 70% confluence at 37˚C. Subsequently, transfection with a final concentration of 50 nM shRNA and/or 15 nM overexpression vectors was performed using the Lipofectamine® 2000 (Invitrogen; Thermo Fisher Scientific, Inc.) for 48 h at 37˚C as per the manufacturer's instructions. At 48 h after transfection, transfection efficiency was evaluated by reverse transcription-quantitative PCR (RT-qPCR) and western blot analysis.

Cell viability assay. The viability of SAOS-2 cells was tested using Cell Counting Kit-8 (CCK-8; Beijing Solarbio Science & Technology Co., Ltd.) assay according to the manufacturer's protocol. Following transfection, SAOS-2 cells were plated in 96-well plates at a density of $1x10^4$ cells/well for 24, 48 and 72 h at 37˚C. Then, at the end of each incubation time point, the 10 μl CCK-8 solution was added to each well. The absorbance at 450 nm was detected using a microplate reader (Agilent Technologies, Inc.) following incubation with CCK-8 solution for 4 h.

Colony formation assay. The proliferation of SAOS-2 cells after transfection was determined by colony formation assay. Briefly, SAOS-2 cells (500 cells/well) were seeded in 6-well plates. Following incubation in RPMI-1640 medium at 37˚C for 2 weeks, cells were fixed with methanol at room temperature for 30 min and stained with 0.5% crystal violet solution for 30 min at room temperature. Colonies (>50 cells) were counted manually in five fields of view using an inverted light microscope (Olympus Corporation; magnification, x10).

Cell apoptosis analysis. TUNEL assay kit (Invitrogen; Thermo Fisher Scientific, Inc.) was used to assess cell apoptosis according to the manufacturer's instructions. Fixation and permeabilization of SAOS-2 cells were performed with 4% paraformaldehyde at room temperature for 15 min and 0.25% Triton-X 100 for 20 min at room temperature, respectively. Subsequently, cells were labeled with TUNEL at 37˚C for 1 h, mounted with Vectashield® mounting medium containing 1 mg/ml DAPI at 37˚C for 10 min away from light. Finally, images of the positive apoptotic cells were acquired with a fluorescence microscope (Olympus Corporation; magnification, x200) in five random fields and quantified by ImageJ software (v1.8.0; National Institutes of Health).

Transwell invasion assay. To evaluate invasion of SAOS-2 cells, the upper chamber of a Transwell chamber (Becton, Dickinson and Company) with an 8-μm pore size was pre-coated with Matrigel (Corning, Inc.) at 37˚C for 1 h. A total of $5x10^4$ cells suspended in serum-free RPMI-1640 medium (HyClone; Cytiva) were seeded in the upper chamber. The lower chamber was filled with 600 μl RPMI-1640 medium (HyClone; Cytiva) containing 10% FBS (Gibco; Thermo Fisher Scientific, Inc.). After 24 h at 37˚C, invaded cells were fixed using 4% paraformaldehyde at room temperature for 30 min and stained with 0.1% crystal violet at room temperature for 20 min. Images of invasive cells were taken by a light microscope (Olympus Corporation) at a magnification of x100.

Wound healing assay. The migratory ability of SAOS-2 cells was assessed via wound healing assay. Transfected SAOS-2 cells were incubated in 6-well plates using serum-free RPMI-1640 medium (HyClone; Cytiva) at 37˚C for 24 h until cells reached 90% confluence. Subsequently, uniform wounds were scraped with a 200-μl sterile tip across the monolayer of cells. PBS was used to remove cell debris. Then, the medium was replaced with serum-free RPMI-1640 medium (HyClone; Cytiva) and cells were cultured at 37˚C for 24 h. Images at 0 and 24 h after wounding were captured by a light microscope (Olympus Corporation) at a magnification of x100. The distance of cell migration was quantified using the following equation: Migration (%)=[(0 h average scratch distance-24 h average scratch distance)/0 h average scratch distance] x100.

Co-immunoprecipitation (Co-IP) assay. SAOS-2 cells were lysed in RIPA buffer (Protech Technology Enterprise Co.,

Ltd.) including protease inhibitors at 4°C to obtain the protein. Subsequently, samples (250 μl) were incubated overnight at 4°C with IgG (1:50; cat. no. ab172730; Abcam), anti-APOC1 (1:40; ab198288; Abcam) or anti-MTCH2 antibodies (1:50; 16888-1-AP; Proteintech). A total of 30 μl protein A/G magnetic beads (MilliporeSigma) was added and incubated overnight at 4°C. The beads were washed with PBS and immunoprecipitants were assessed via western blotting.

Measurement of glucose metabolism. Seahorse XF Cell Mito Stress Test kit (Agilent Technologies, Inc.) was used to determine the O_2 consumption rate (OCR) and Seahorse XF Glycolysis Stress Test kit was used to examine the extracellular acidification rate (ECAR), as previously described (19). The transfected SAOS-2 cells ($1x10^5$) were plated onto a Seahorse XF-96 cell culture microplate. Cells were next equilibrated with XF Base media (Agilent Technologies Deutschland GmbH) at 37°C for 1 h in an incubator lacking CO_2 and then serum-starved for 1 h in glucose-free media-containing treatments (Invitrogen; Thermo Fisher Scientific, Inc.). A total of 1 mM oligomycin, 1 mM p-trifluoromethoxy carbonyl cyanide phenylhydrazone (MilliporeSigma), 2 mM antimycin A (MilliporeSigma) and 2 mM rotenone (MilliporeSigma) were added to each well at 37°C overnight to detect the OCR. For the measurement of ECAR, each well contained 10 mM glucose, 1 mM oligomycin (MilliporeSigma) and 80 mM 2-deoxyglucose (MilliporeSigma) at 37°C overnight. A Seahorse XF-96 analyzer (Agilent Technologies, Inc.) was used to detect the samples and data were assessed using Seahorse XFe24 Wave version 2.2 software (Agilent Technologies, Inc.).

Detection of lactate production. The generation of lactate in SAOS-2 cells in a 96-well plate at a density of $5x10^3$ cells per well following transfection was examined using a lactate assay kit (cat. no. A020-2-2; Nanjing Jiancheng Bioengineering Institute), according to the manufacturer's protocol. All values were normalized to cellular protein level.

Phosphofructokinase (PFK), pyruvate kinase (PK) and hexokinase (HK) activity measurement. Cells were seeded into 6-well plates at a density of $2x10^6$ cells/well. By using PFK (cat. no. A129-1-1), PK (cat. no. A076-1-1) and HK (cat. no. A077-3-1) assay kit provided by Nanjing Jiancheng Bioengineering Institute, the levels of PFK, PK and HK were estimated according to the manufacturer's protocols.

RT-qPCR. Total RNA was isolated from HOS, SAOS-2, 143B, U2OS and hFOB1.19 cells using TRIzol® (Invitrogen; Thermo Fisher Scientific, Inc.). RNA quality was assessed using a NanoDrop™ 2000 spectrophotometer (Thermo Fisher Scientific, Inc.). RNA samples with A260/A280 ratio between 1.8 and 2.0 were used in RT to synthesize complementary DNA (cDNA). RT was performed to generate cDNA using the PrimeScript RT reagent kit (Takara Biotechnology Co., Ltd.), according to the manufacturer's protocol. The detection of mRNA expression was performed in an ABI 7500 system (Applied Biosystems; Thermo Fisher Scientific, Inc.) with a QuantiNova® SYBR® Green PCR kit (Qiagen GmbH). The following thermocycling conditions were used: Initial denaturation at 95°C for 10 min; followed by 35 cycles of denaturation at 95°C for 15 sec, annealing at 60°C for 1 min and extension of 10 min at 65°C. Primers pairs used in the present study were as follows: APOC1 forward, 5'-CTGAGT GGGGAAAGGGACTA-3' and reverse, 5'-GGAGGGGCA CTCTCTCAATC-3'; MTCH2 forward, 5'-AAAGTGCTC ATCCAGGTGGG-3' and reverse, 5'-ACCACAGTTGTTGAC AGCCA-3' and GAPDH forward, 5'-GGAGCGAGATCCCTC CAAAAT-3' and reverse, 5'-GGCTGTTGTCATACTTCT CATGG-3'. Results were represented as fold induction using the $2^{-\Delta\Delta Cq}$ method (22). Primers were commercially synthesized by Shanghai GenePharma Co., Ltd. GAPDH served as an internal reference.

Western blot analysis. Protein was extracted from HOS, SAOS-2, 143B, U2OS and hFOB1.19 cells using RIPA lysis buffer (Beyotime Institute of Biotechnology) and protein concentrations were quantified using a BCA kit (Beyotime Institute of Biotechnology). An equal amount of cell extract (35 μg/lane) was electrophoresed on 12% SDS-PAGE. The proteins were transferred to PVDF membranes (MilliporeSigma). Next, the membranes were blocked for 1 h at room temperature in 5% lipid-free milk solution. Following incubation with primary antibodies diluted in TBS-0.1% Tween-20 (TBST) overnight at 4°C, the membranes were washed thrice with 0.1% TBST for 10 min each and incubated with goat anti-rabbit horseradish peroxidase-conjugated secondary antibody (cat. no. 7074; 1:5,000; Cell Signaling Technology, Inc.) for 1 h at room temperature. ECL reagent (Pierce; Thermo Fisher Scientific, Inc.) and the enhanced chemiluminescence detection system (MilliporeSigma) were used to perform visualization. Protein bands on the membrane were quantified using ImageJ Software (v1.8.0; National Institutes of Health). GAPDH was used as the loading control. The following primary antibodies were used: Anti-APOC1 (cat. no. ab198288; 1:1,000; Abcam), anti-MTCH2 (cat. no. 16888-1-AP; 1:1,000; ProteinTech Group, Inc.), anti-Bcl-2 (cat. no. 4223T; 1:1,000; Cell Signaling Technology, Inc.), anti-Bax (cat. no. 41162S; 1:1,000; Cell Signaling Technology, Inc.), anti-cleaved-caspase 3 (cat. no. 9664T; 1:1,000; Cell Signaling Technology, Inc.), anti-caspase 3 (cat. no. 14220T; 1:1,000; Cell Signaling Technology, Inc.), anti-matrix metallopeptidase (MMP)2 (cat. no. 40994S; 1:1,000; Cell Signaling Technology, Inc.), anti-MMP9 (cat. no. 13667T; 1:1,000; Cell Signaling Technology, Inc.) and anti-GAPDH (cat. no. 5174T; 1:1,000; Cell Signaling Technology, Inc.) antibodies were utilized.

Statistical analysis. Data from three independent replicates are presented as the mean ± standard deviation and were analyzed using GraphPad Prism version 8.0 (GraphPad Software, Inc.). Unpaired student's t-test was used to analyze the means of two groups. One-way ANOVA followed by Tukey's post-hoc test was used for comparisons between >2 groups. $P<0.05$ was considered to indicate a statistically significant difference.

Results

APOC1 is highly expressed in osteosarcoma cells and APOC1 silencing inhibits proliferation and promotes apoptosis of osteosarcoma cells. Osteosarcoma (HOS, SAOS-2, 143B and U2OS) and human osteoblast cell line hFOB1.19 were used to evaluate

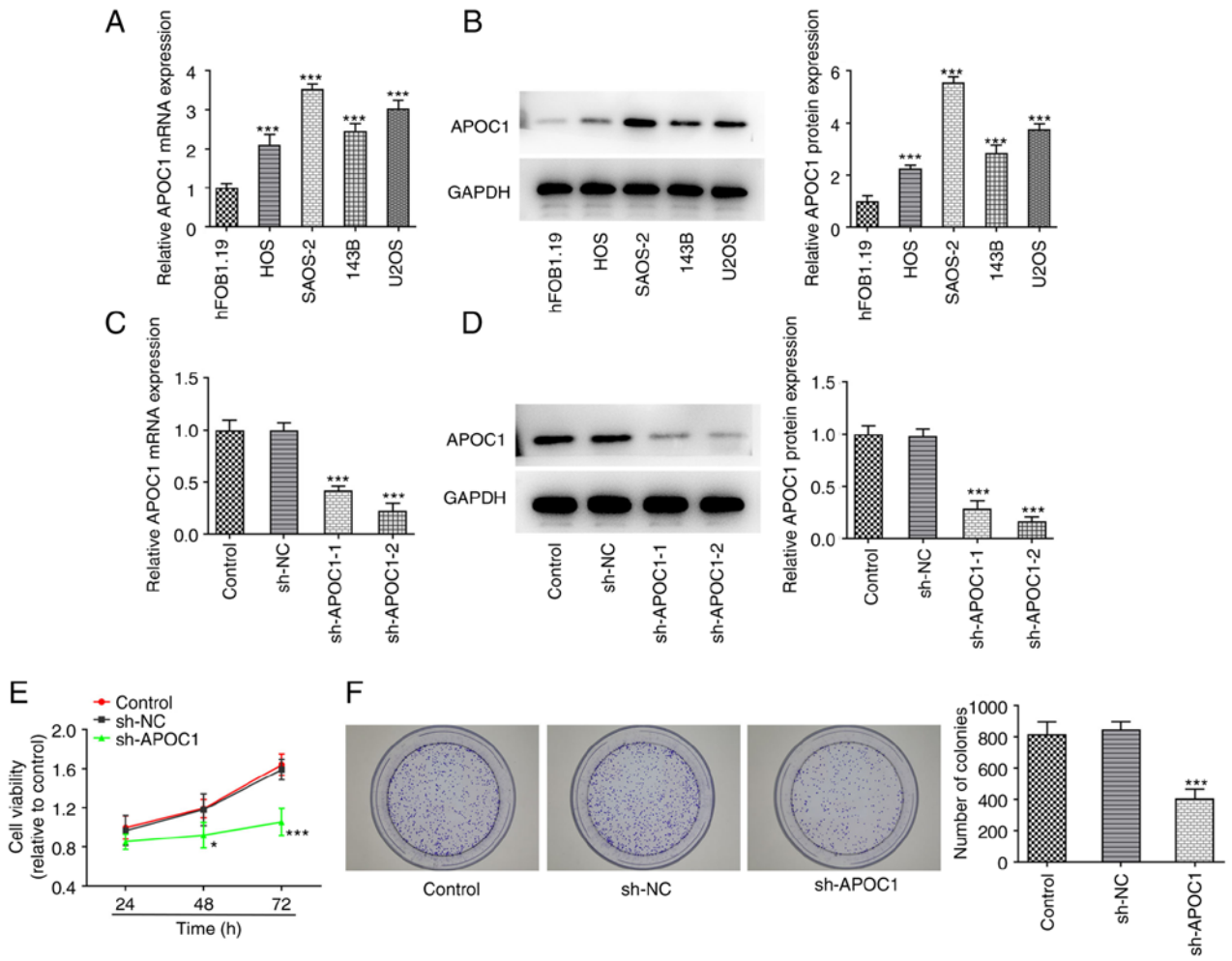

Figure 1. APOC1 expression is significantly elevated in osteosarcoma cells and APOC1 silencing inhibits proliferation of osteosarcoma cells. Evaluation of APOC1 expression in osteosarcoma (HOS, SAOS-2, 143B and U2OS) and human osteoblast cell line hFOB1.19 using (A) RT-qPCR and (B) western blotting. ***P<0.001 vs. hFOB1.19. Assessment of APOC1 expression in SAOS-2 cells after transfection with sh-APOC1-1 or sh-APOC1-2 by (C) RT-qPCR and (D) western blotting. (E) Cell viability was tested by Cell Counting Kit-8 assay. (F) Proliferation of SAOS-2 cells was examined by colony formation assay. Magnification, x10. *P<0.05, ***P<0.001 vs. sh-NC. APOC1, apolipoprotein C1; RT-qPCR, reverse transcription-quantitative PCR; sh, short hairpin; NC, negative control.

expression of APOC1. APOC1 expression was significantly upregulated in these osteosarcoma cell lines compared with the hFOB1.19 cell line (Fig. 1A and B). The highest APOC1 expression was exhibited in SAOS-2 cells. Therefore, this cell line was selected for subsequent experiments. APOC1 was silenced to investigate the role of APOC1 in the proliferation and apoptosis of SAOS-2 cells. APOC1 expression was significantly downregulated in both sh-APOC1-1 and sh-APOC1-2 groups when compared with the sh-NC group (Fig. 1C and D). sh-APOC1-2 possessed the better knockdown efficiency and was selected for subsequent experiments. Results of the CCK-8 assay suggested that the activity of SAOS-2 cells was significantly decreased after APOC1 silencing compared with the sh-NC group at 48 and 72 h (Fig. 1E). Consistently, colony formation assay indicated that APOC1 deletion inhibited cell proliferation compared with the sh-NC group (Fig. 1F). SAOS-2 cells transfected with sh-APOC1 showed increased apoptotic capacity compared with those transfected with sh-NC (Fig. 2A). Western blot analysis suggested that APOC1 silencing led to significant downregulation of Bcl-2 expression and upregulation in Bax and cleaved-caspase 3 expression (Fig. 2B). The aforementioned data revealed that APOC1 knockdown suppressed the proliferation and increased apoptosis of osteosarcoma cells.

APOC1 silencing suppresses invasion and migration of osteosarcoma cells. Transwell and wound healing assays were used to determine the invasive and migratory ability of SAOS-2 cells following APOC1 deletion. APOC1 knockdown significantly inhibited the invasion and migration of SAOS-2 cells relative to the sh-NC group (Fig. 3A and B). Expression of migration-associated proteins MMP2 and MMP9 was also downregulated in cells transfected with sh-APOC1 (Fig. 3C). These findings indicated that APOC1 deletion inhibited invasion and migration of osteosarcoma cells.

APOC1 interacts with MTCH2 in osteosarcoma cells. To explore the potential mechanism by which APOC1 regulates malignant biological behaviors of osteosarcoma cells, BioGRID and STRING databases were used to analyze the proteins that may interact with APOC1. MTCH2 was noted to interact with APOC1 (Fig. 4A and B). Compared with hFOB1.19 cells, significantly elevated MTCH2 mRNA and protein expression levels were

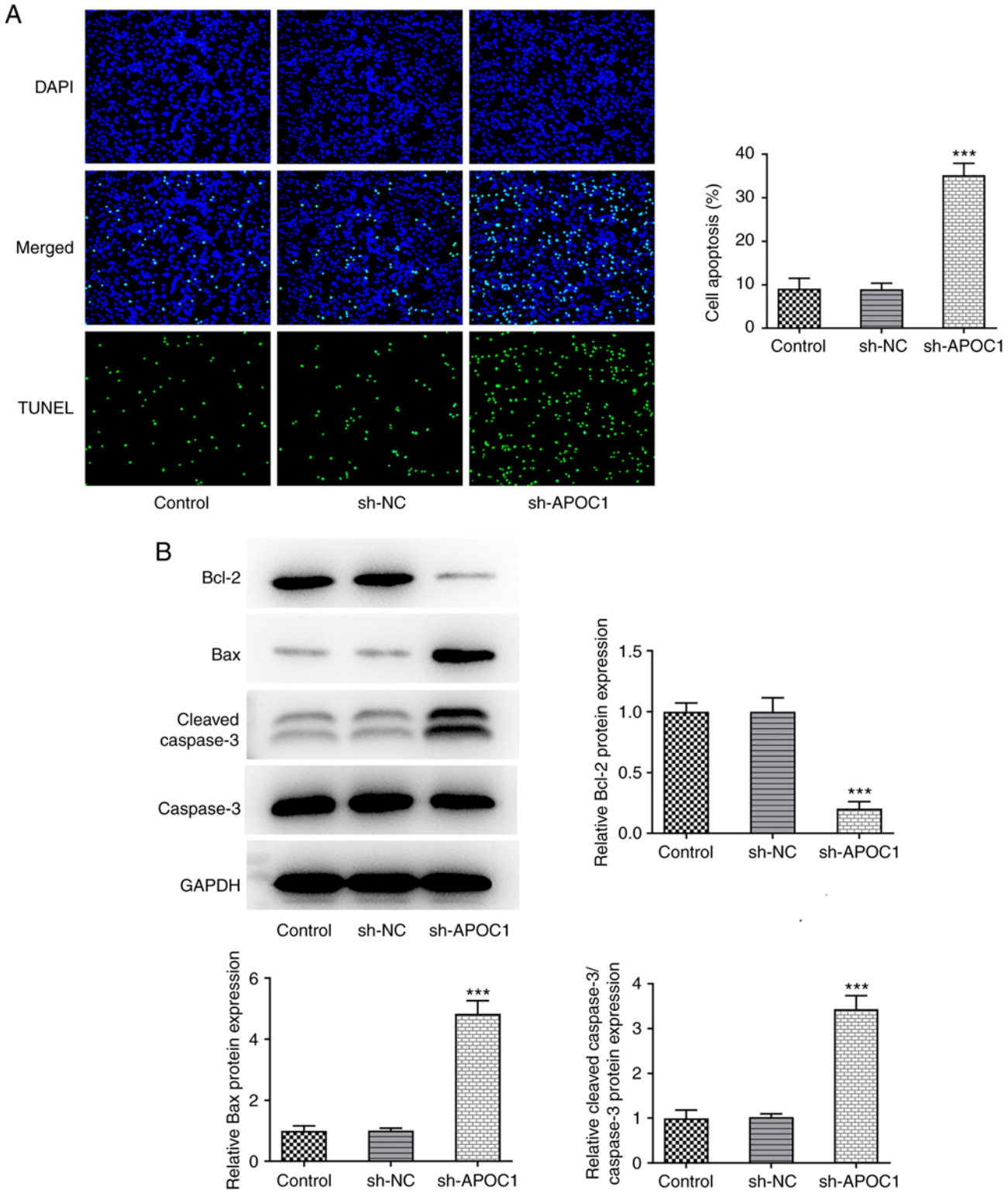

Figure 2. APOC1 silencing promotes apoptosis of osteosarcoma cells. (A) Cell apoptosis was detected using TUNEL staining. Magnification, x200. (B) Western blot analysis was to measure apoptosis-related protein expression. ***P<0.001 vs. sh-NC. APOC1, apolipoprotein C1; sh, short hairpin; NC, negative control.

observed in SAOS-2 cells (Fig. 4C and D). APOC1 could bind with MTCH2 (Fig. 4E). These results validated the prediction that APOC1 interacted with MTCH2 in osteosarcoma.

MTCH2 upregulation inhibits the effect of APOC1 deletion on the malignant behavior of osteosarcoma cells. The present study investigated whether the inhibitory effect of APOC1 on osteosarcoma was achieved by regulating MTCH2. MTCH2 was overexpressed by transfection with MTCH2 pcDNA3.1 plasmid, resulting in significantly upregulated MTCH2 expression (Fig. 5A and B). Viability and cell proliferation were elevated in SAOS-2 cells co-transfected with sh-APOC1 and Oe-MTCH2 compared with the sh-APOC1 + Oe-NC group (Fig. 5C and D). Additionally, TUNEL staining indicated that

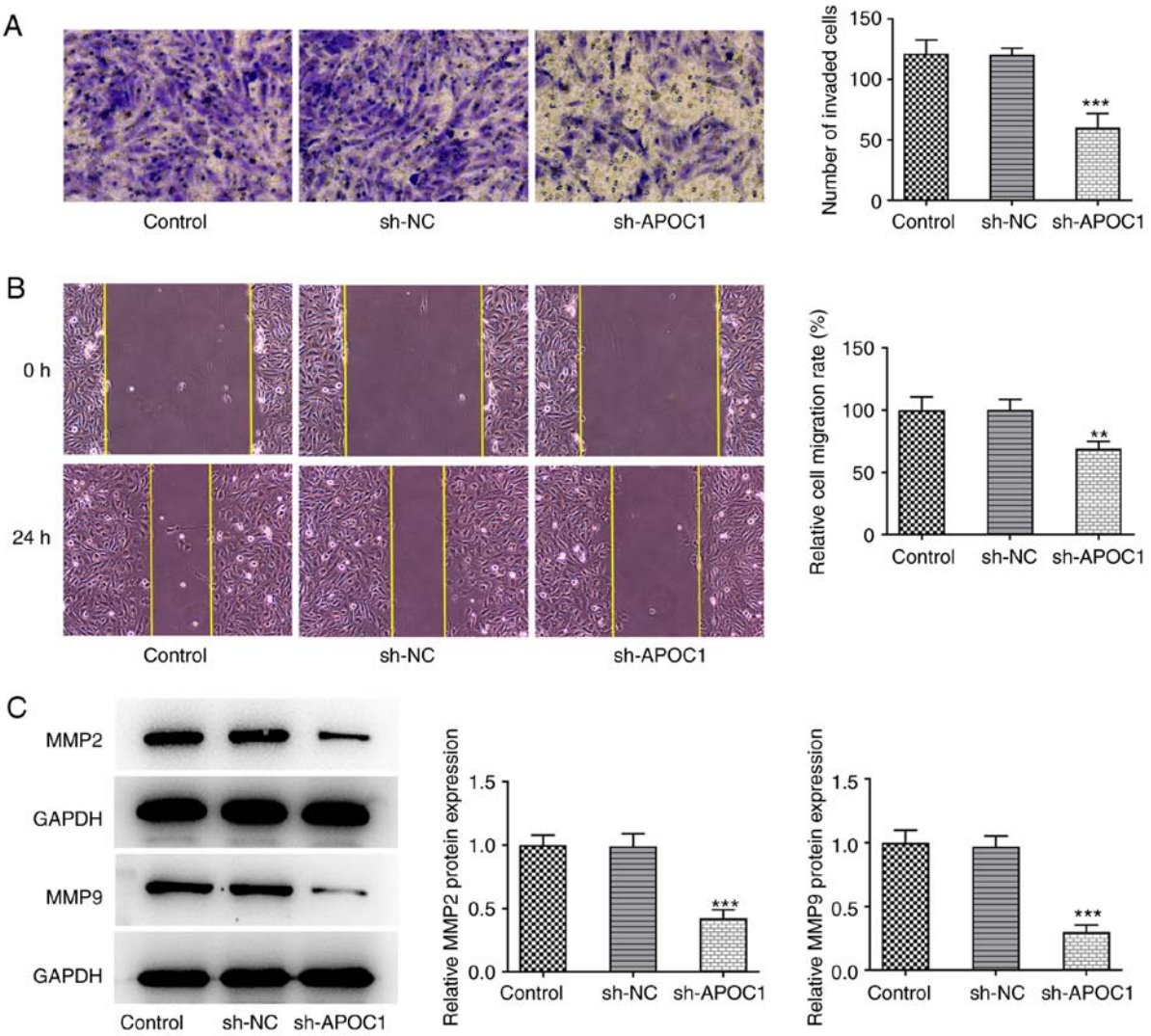

Figure 3. APOC1 silencing suppresses invasion and migration of osteosarcoma cells. (A) Invasion of SAOS-2 cells was determined by Transwell assay. Magnification, x100. (B) Wound healing assay was used to estimate cell migration. Magnification, x100. (C) Expression of MMP2 and MMP9 was detected by western blotting. **P<0.01, ***P<0.001 vs. sh-NC. APOC1, apolipoprotein C1; MMP, matrix metallopeptidase; sh, short hairpin; NC, negative control.

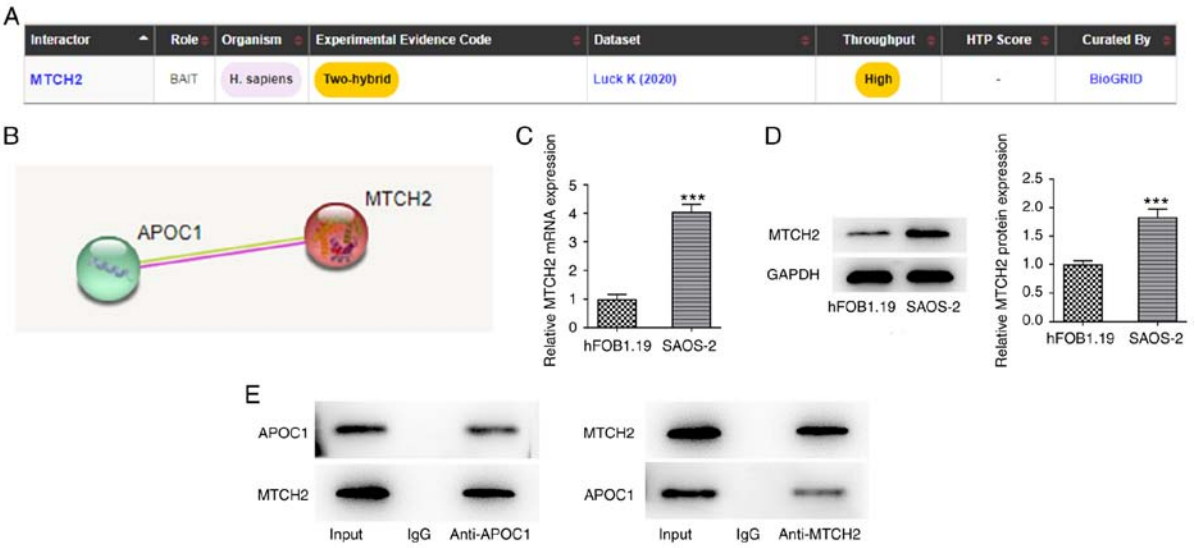

Figure 4. APOC1 may interact with MTCH2 in osteosarcoma. (A) BioGRID and (B) STRING databases predicted that APOC1 interacted with MTCH2. Measurement of MTCH2 expression in SAOS-2 and hFOB1.19 cells by (C) reverse transcription-quantitative PCR and (D) western blotting. ***P<0.001 vs. hFOB1.19. (E) Verification of the interaction between APOC1 and MTCH2 using co-immunoprecipitation assay. APOC1, apolipoprotein C1; MTCH2, mitochondrial carrier homolog 2.

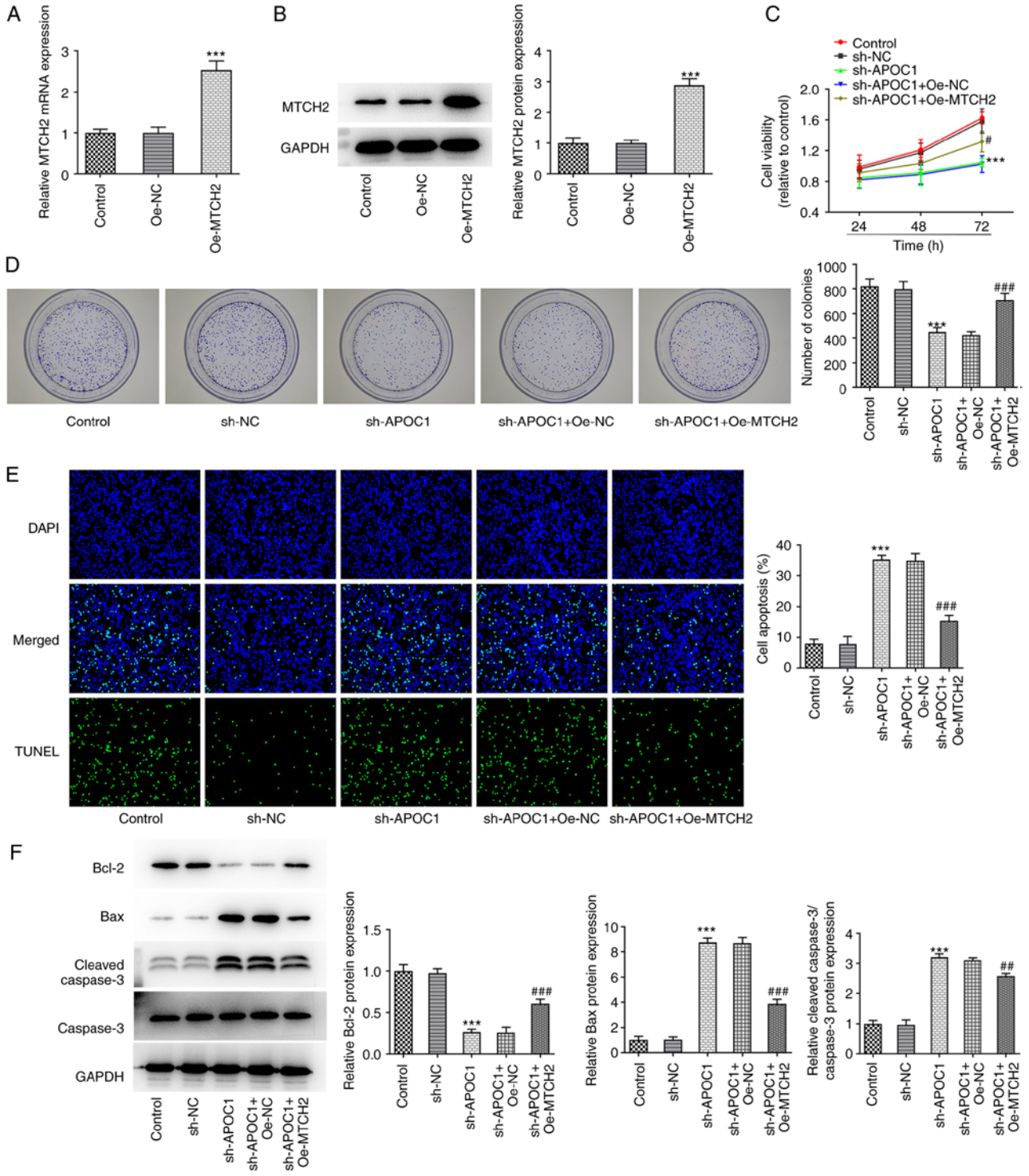

Figure 5. MTCH2 overexpression inhibits the effect of APOC1 deletion on the proliferation and apoptosis of osteosarcoma cells. Expression of MTCH2 after transfection with Oe-MTCH2 was detected using (A) reverse transcription-quantitative PCR and (B) western blotting. ***P<0.001 vs. Oe-NC. (C) Cell viability was analyzed by Cell Counting Kit-8 assay. (D) Colony formation assay was used for the detection of cell proliferation. Magnification, x10. (E) Cell apoptosis was tested using TUNEL staining. Magnification, x200. (F) Expression of apoptosis-related proteins was estimated using western blotting. ***P<0.001 vs. sh-NC; #P<0.05, ##P<0.01, ###P<0.001 vs. sh-APOC1 + Oe-NC. MTCH2, mitochondrial carrier homolog 2; APOC1, apolipoprotein C1; Oe, overexpression; NC, negative control; sh, short hairpin.

MTCH2 overexpression significantly decreased the apoptosis of SAOS-2 cells transfected with sh-APOC1 (Fig. 5E). Consistently, MTCH2 upregulation significantly increased Bcl-2 expression and decreased Bax and cleaved-caspase 3 expression compared with the sh-APOC1 + Oe-NC group (Fig. 5F). Furthermore, in the sh-APOC1 + Oe-MTCH2 group, the invasion and migration of SAOS-2 cells were significantly enhanced compared with the sh-APOC1 + Oe-NC group, coupled with significantly upregulated MMP2 and MMP9 expression (Fig. 6A-C). Together, these findings confirmed that APOC1 regulated development of osteosarcoma by binding to MTCH2.

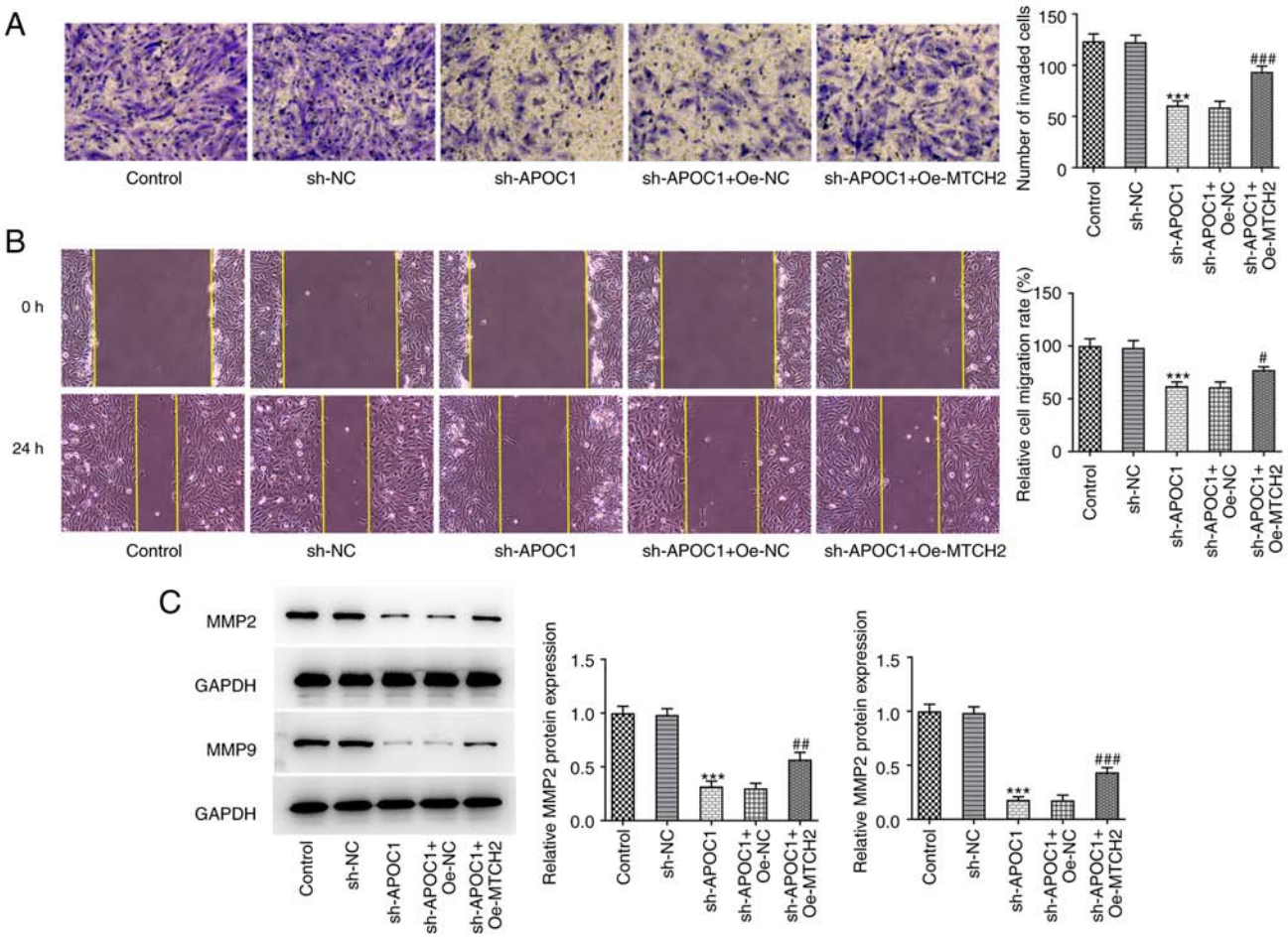

Figure 6. MTCH2 overexpression attenuates the effects of APOC1 knockdown on invasion and migration of osteosarcoma cells. (A) Invasion of SAOS-2 cells was evaluated by Transwell assay. Magnification, x100. (B) Wound healing assay was used for measurement of cell migration. Magnification, x100. (C) Expression of MMP2 and MMP9 was determined using western blotting. ***P<0.001 vs. sh-NC; $^{\#}$P<0.05, $^{\#\#}$P<0.01, $^{\#\#\#}$P<0.001 vs. sh-APOC1 + Oe-NC. MTCH2, mitochondrial carrier homolog 2; APOC1, apolipoprotein C1; MMP, matrix metallopeptidase; sh, short hairpin; NC, negative control; Oe, overexpression.

APOC1 silencing promotes OXPHOS and inhibits the Warburg effect of osteosarcoma cells by regulating MTCH2 expression. Previous studies have suggested that the Warburg effect serves a key role in proliferation of osteosarcoma cells (23,24). The effects of APOC1 silencing on OXPHOS and the Warburg effect of SAOS-2 cells were analyzed. knockdown significantly elevated the basal and maximal OCR (the marker of OXPHOS) (25) in SAOS-2 cells compared with the sh-NC group up to 60 min (Fig. 7A). By contrast, Oe-MTCH2 transfection reversed the elevated OCR caused by APOC1 silencing. ECAR was significantly reduced up to 60 min in SAOS-2 cells transfected with sh-APOC1, whereas MTCH2 overexpression alleviated this effect (Fig. 7B). APOC1 knockdown led to decreased lactate production in SAOS-2 cells relative to the sh-NC group, which was reversed by Oe-MTCH2 transfection (Fig. 7C). Activities of key enzymes involved in glycolysis, including HK, PFK and PK, were significantly decreased in SAOS-2 cells following APOC1 silencing compared with the sh-NC group (Fig. 7D-F). Conversely, MTCH2 overexpression inhibited the impacts of APOC1 silencing alone on levels of these key enzymes. The aforementioned observations demonstrated that APOC1 regulated OXPHOS and the Warburg effect of osteosarcoma cells by binding to MTCH2.

Discussion

Although osteosarcoma, a high-mortality cancerous tumor located at the end of the metaphysis, can affect people of any age, it is typically diagnosed in children and adolescents (26). New therapies are urgently needed because of the poor 5-year survival rate despite application of current treatment strategies for osteosarcoma. The present study investigated the role of APOC1 in the development of osteosarcoma and its regulatory effect on MTCH2 to delineate the detailed molecular mechanisms underlying the pathogenesis of osteosarcoma.

APOC1 is a polypeptide of 57 amino acid residues that is primarily synthesized in the liver and secreted into serum in an autocrine manner (27). It participates in lipoprotein metabolism by regulating activity of enzymes associated with intravascular lipoprotein metabolism (28,29). A growing body of literature has shown that APOC1 is involved in multiple biological processes, such as cholesterol catabolism, dendritic reorganization and membrane remodeling (30,31). Recently, APOC1 has been reported to be associated with occurrence and prognosis of the majority of cancers, such as cervical cancer, renal cell carcinoma and breast and esophageal cancer (8,9,32,33). Takano *et al* (34) demonstrated that

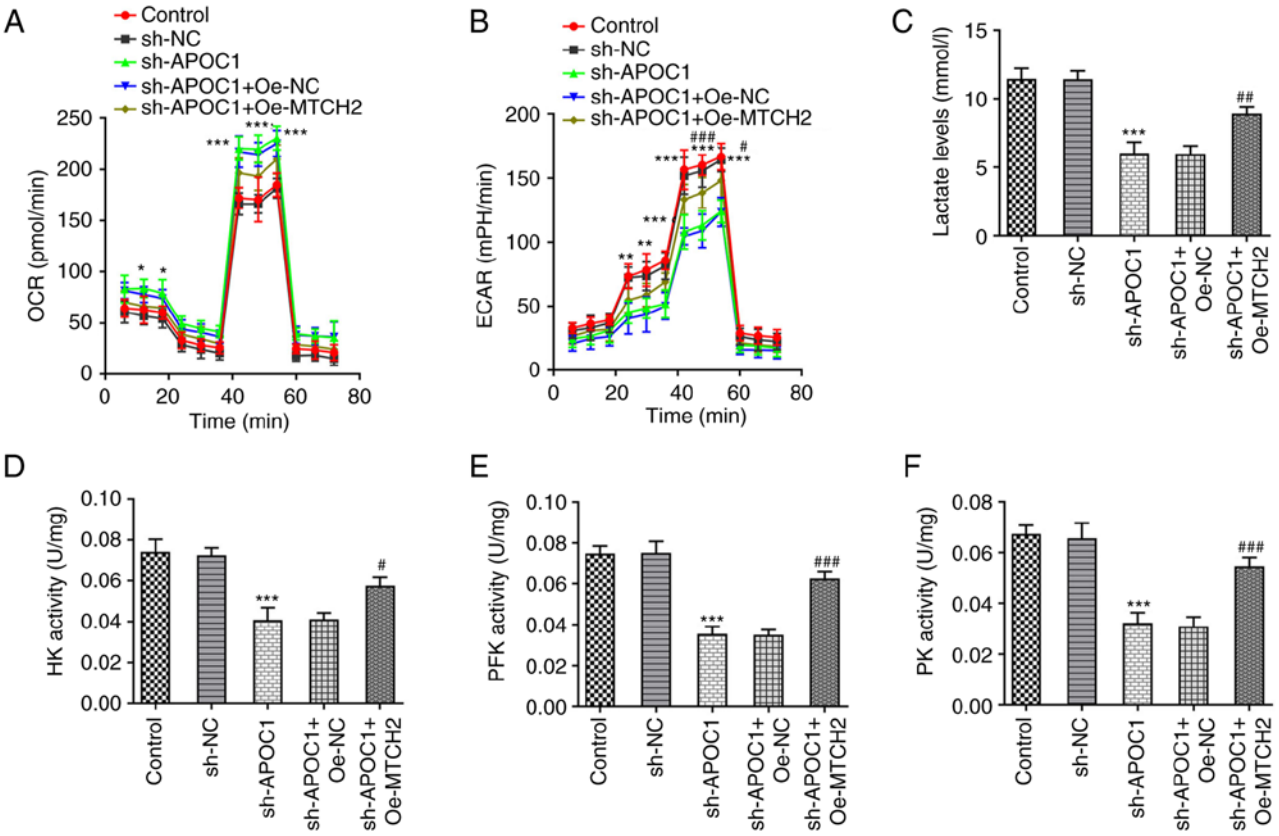

Figure 7. APOC1 silencing promotes oxidative phosphorylation and inhibits the Warburg effect of osteosarcoma cells by regulating MTCH2 expression. (A) OCR of SAOS-2 cells was detected using the Seahorse XF Cell Mito Stress Test kit. (B) ECAR was assessed using the Seahorse XF Glycolysis Stress Test kit. (C) Lactate production was tested using lactate assay kit. Corresponding commercially available kits were used to measure the activity of (D) HK, (E) PFK and (F) PK. *P<0.05, **P<0.01, ***P<0.001 vs. sh-NC; $^{\#}$P<0.05, $^{\#\#}$P<0.01, $^{\#\#\#}$P<0.001 vs. sh-APOC1 + Oe-NC. APOC1, apolipoprotein C1; MTCH2, mitochondrial carrier homolog 2; OCR, O_2 consumption rate; ECAR, extracellular acidification rate; HK, hexokinase; PFK, phosphofructokinase; PK, pyruvate kinase; sh, short hairpin; NC, negative control; Oe, overexpression.

APOC1 can maintain cell survival by inhibiting apoptosis of pancreatic cancer cells. Downregulation of APOC1 elicits inhibitory effects on proliferation, invasion and migration of colorectal cancer cells (7). Similarly, Wang *et al* (35) showed that APOC1 is highly expressed in clear cell renal cell carcinoma tissue and APOC1 knockdown suppresses cell proliferation, invasion and migration. Moreover, evidence has indicated that knockdown of APOC1 in osteosarcoma significantly inhibits tumor cell proliferation (36). Also, as noted by Liu *et al* (10) using the analysis of gene expression profiles, APOC1 expression is continuously upregulated in osteosarcoma tissue samples during the occurrence and metastasis of osteosarcoma. Bcl-2 is an integral membrane protein that is primarily located on the outer membrane of mitochondria and induces release of caspase-3, which serves as an executioner to facilitate cell death (37). Proteins in the Bcl-2 family exhibit either pro-apoptotic or anti-apoptotic activities, with Bcl-2 and Bax serving as markers to determine cell susceptibility to apoptosis (38,39). In addition, the Bcl-2/Bax signaling pathway has been shown to participate in apoptosis in osteosarcoma (40,41). MMP2 and MMP9 are expressed in cancer cells during malignant invasion and migration and are proteolytic enzymes that degrade the extracellular matrix and induce cancer cells to permeate the basement membrane (42). Detection of alterations in proliferative, apoptotic, invasive and migratory abilities are commonly used to assess the effects of novel oncogenes on tumors. Consistent with the aforementioned studies, the present study also found that APOC1 served as a cancer-promoting gene in osteosarcoma and APOC1 silencing inhibited the progression of osteosarcoma by preventing proliferation, invasion and migration and inducing apoptosis.

By using the BioGRID and STRING databases, it was found that MTCH2 was a potential protein that may interact with APOC1. MTCH2 is a 33 kDa protein localized in the mitochondrial outer membrane (43,44). Studies imply that MTCH2 is involved in the pathogenesis of numerous types of tumors (13,45,46). For example, CRISPR screening has identified MTCH2 as key for the proliferation and viability of leukemia cells and MTCH2 deletion decreases proliferation and promotes the differentiation of acute myeloid leukemia cells (45). Emerging evidence has shown that MTCH2 knockdown impedes invasion and migration of glioma cells and renders cells susceptible to temozolomide-triggered apoptosis (13). MTCH2 is significantly downregulated in ErbB2-driven breast cancer, the induction of which attenuates tumorigenicity and causes cell cycle arrest in breast cancer (46). A recent study demonstrated elevated MTCH2 expression in osteosarcoma clinical samples, which is the first report about MTCH2 in osteosarcoma (12). In line with findings by Fu *et al* (12), in the present study, MTCH2 was highly expressed in osteosarcoma cells. Co-IP assay confirmed that

APOC1 interacted with MTCH2 in SAOS-2 cells. Functional experiments further revealed that MTCH2 upregulation inhibited the impact of APOC1 deletion on the malignant behavior of osteosarcoma cells, suggesting that APOC1 affected osteosarcoma tumor progression via MTCH2.

Glycolysis is a key hallmark of cancerous tissues because cancer cells use energy through glycolysis rather than the tricarboxylic acid cycle to obtain sufficient energy to proliferate, migrate and metastasize (21,47). The Warburg effect, which is the metabolic shift from energy acquisition primarily through balanced mitochondrial OXPHOS to fast but inefficient aerobic glycolysis, is hypothesized to be an important driver of tumor formation and proliferation (15). HK, PFK and PK, key enzymes in glycolysis, serve important roles in glycolytic metabolism (48,49). Osteosarcoma has a strong glycolytic phenotype and studies have shown that aberrantly expressed molecules, including c-Myc, SLIT2 and ROBO1, in osteosarcoma can inhibit mitochondrial OXPHOS and promote aerobic glycolysis (50-52). MTCH2 is a suppressor of mitochondrial metabolism in the hematopoietic system and MTCH2 deletion promotes mitochondrial OXPHOS (53). The present study showed that MTCH2 upregulation restored the impact of APOC1 on OCR, ECAR, lactate production and HK, PFK and PK activities in SAOS-2 cells, demonstrating that APOC1 regulated OXPHOS and the Warburg effect of osteosarcoma cells by binding to MTCH2.

However, the present study has a limitation. In the present study, only the regulatory effect of APOC1 and MTCH2 on progression of SAOS-2 cells was discussed. Therefore, further *in vivo* experiments involving transgenic animals need to be performed to support the present conclusions.

Taken together, the aforementioned findings elucidated that APOC1, a potential tumor oncogenic protein, performs its functions by binding with MTCH2. APOC1/MTCH2 may be a novel therapeutic target for osteosarcoma treatment. The present study may also provide novel insights into the mechanisms of osteosarcoma carcinogenesis.

Acknowledgements

Not applicable.

Funding

No funding was received.

Availability of data and materials

The datasets used and/or analyzed during the current study are available from the corresponding author on reasonable request.

Authors' contributions

RL and XH designed the study. RL and HH performed the experiments and analyzed the data. XH drafted the manuscript and interpreted data. RL revised the manuscript for important intellectual content. All authors have read and approved the final manuscript. RL and XH confirm the authenticity of all the raw data.

Ethics approval and consent to participate

Not applicable.

Patient consent for publication

Not applicable.

Competing interests

The authors declare that they have no competing interests.

References

1. Gianferante DM, Mirabello L and Savage SA: Germline and somatic genetics of osteosarcoma-connecting aetiology, biology and therapy. Nat Rev Endocrinol 13: 480-491, 2017.
2. Whelan JS and Davis LE: Osteosarcoma, chondrosarcoma, and chordoma. J Clin Oncol 36: 188-193, 2018.
3. Zheng Y, Wang G, Chen R, Hua Y and Cai Z: Mesenchymal stem cells in the osteosarcoma microenvironment: Their biological properties, influence on tumor growth, and therapeutic implications. Stem Cell Res Ther 9: 22, 2018.
4. Anderson ME: Update on survival in osteosarcoma. Orthop Clin North Am 47: 283-292, 2016.
5. Brewer HB Jr, Shulman R, Herbert P, Ronan R and Wehrly K: The complete amino acid sequence of alanine apolipoprotein (apoC-3), and apolipoprotein from human plasma very low density lipoproteins. J Biol Chem 249: 4975-4984, 1974.
6. Fuior EV and Gafencu AV: Apolipoprotein C1: Its pleiotropic effects in lipid metabolism and beyond. Int J Mol Sci 20: 5939, 2019.
7. Ren H, Chen Z, Yang L, Xiong W, Yang H, Xu K, Zhai E, Ding L, He Y and Song X: Apolipoprotein C1 (APOC1) promotes tumor progression via MAPK signaling pathways in colorectal cancer. Cancer Manag Res 11: 4917-4930, 2019.
8. Shi X, Wang J, Dai S, Qin L, Zhou J and Chen Y: Apolipoprotein C1 (APOC1): A novel diagnostic and prognostic biomarker for cervical cancer. Onco Targets Ther 13: 12881-12891, 2020.
9. Guo Q, Liu XL, Jiang N, Zhang WJ, Guo SW, Yang H, Ji YM, Zhou J, Guo JL, Zhang J and Liu HS: Decreased APOC1 expression inhibited cancer progression and was associated with better prognosis and immune microenvironment in esophageal cancer. Am J Cancer Res 12: 4904-4929, 2022.
10. Liu J, Wu S, Xie X, Wang Z and Lei Q: Identification of potential crucial genes and key pathways in osteosarcoma. Hereditas 157: 29, 2020.
11. Robinson AJ, Kunji ER and Gross A: Mitochondrial carrier homolog 2 (MTCH2): The recruitment and evolution of a mitochondrial carrier protein to a critical player in apoptosis. Exp Cell Res 318: 1316-1323, 2012.
12. Fu D, Liu S, Liu J, Chen W, Long X, Chen X, Zhou Y, Zheng Y and Huang S: iTRAQ-based proteomic analysis of the molecular mechanisms and downstream effects of fatty acid synthase in osteosarcoma cells. J Clin Lab Anal 35: e23653, 2021.
13. Yuan Q, Yang W, Zhang S, Li T, Zuo M, Zhou X, Li J, Li M, Xia X, Chen M and Liu Y: Inhibition of mitochondrial carrier homolog 2 (MTCH2) suppresses tumor invasion and enhances sensitivity to temozolomide in malignant glioma. Mol Med 27: 7, 2021.
14. Buzaglo-Azriel L, Kuperman Y, Tsoory M, Zaltsman Y, Shachnai L, Zaidman SL, Bassat E, Michailovici I, Sarver A, Tzahor E, *et al*: Loss of muscle MTCH2 increases whole-body energy utilization and protects from diet-induced obesity. Cell Rep 14: 1602-1610, 2016.
15. Vander Heiden MG, Cantley LC and Thompson CB: Understanding the Warburg effect: The metabolic requirements of cell proliferation. Science 324: 1029-1033, 2009.
16. Warburg O, Wind F and Negelein E: The metabolism of tumors in the body. J Gen Physiol 8: 519-530, 1927.
17. Baltazar F, Afonso J, Costa M and Granja S: Lactate beyond a waste metabolite: Metabolic affairs and signaling in malignancy. Front Oncol 10: 231, 2020.
18. Schwartz L, Supuran CT and Alfarouk KO: The Warburg effect and the hallmarks of cancer. Anticancer Agents Med Chem 17: 164-170, 2017.

19. Zhu R, Li X and Ma Y: miR-23b-3p suppressing PGC1α promotes proliferation through reprogramming metabolism in osteosarcoma. Cell Death Dis 10: 381, 2019.
20. Oughtred R, Stark C, Breitkreutz BJ, Rust J, Boucher L, Chang C, Kolas N, O'Donnell L, Leung G, McAdam R, *et al*: The BioGRID interaction database: 2019 update. Nucleic Acids Res 47: D529-D541, 2019.
21. Szklarczyk D, Gable AL, Lyon D, Junge A, Wyder S, Huerta-Cepas J, Simonovic M, Doncheva NT, Morris JH, Bork P, *et al*: STRING v11: Protein-protein association networks with increased coverage, supporting functional discovery in genome-wide experimental datasets. Nucleic Acids Res 47: D607-D613, 2019.
22. Livak KJ and Schmittgen TD. Analysis of relative gene expression data using real-time quantitative PCR and the 2(-Delta Delta C(T)) method. Methods 25: 402-408, 2001.
23. Kobliakov VA: The mechanisms of regulation of aerobic glycolysis (Warburg effect) by oncoproteins in carcinogenesis. Biochemistry (Mosc) 84: 1117-1128, 2019.
24. Abbaszadeh Z, Çeşmeli S and Biray Avcı Ç: Crucial players in glycolysis: Cancer progress. Gene 726: 144158, 2020.
25. Sica V, Bravo-San Pedro JM, Stoll G and Kroemer G: Oxidative phosphorylation as a potential therapeutic target for cancer therapy. Int J Cancer 146: 10-17, 2020.
26. Ottaviani G and Jaffe N: The epidemiology of osteosarcoma. Cancer Treat Res 152: 3-13, 2009.
27. Jong MC, Hofker MH and Havekes LM: Role of ApoCs in lipoprotein metabolism: Functional differences between ApoC1, ApoC2, and ApoC3. Arterioscler Thromb Vasc Biol 19: 472-484, 1999.
28. Jong MC, Dahlmans VE, van Gorp PJ, van Dijk KW, Breuer ML, Hofker MH and Havekes LM: In the absence of the low density lipoprotein receptor, human apolipoprotein C1 overexpression in transgenic mice inhibits the hepatic uptake of very low density lipoproteins via a receptor-associated protein-sensitive pathway. J Clin Invest 98: 2259-2267, 1996.
29. Muurling M, van den Hoek AM, Mensink RP, Pijl H, Romijn JA, Havekes LM and Voshol PJ: Overexpression of APOC1 in obob mice leads to hepatic steatosis and severe hepatic insulin resistance. J Lipid Res 45: 9-16, 2004.
30. Poirier J, Hess M, May PC and Finch CE: Cloning of hippocampal poly(A) RNA sequences that increase after entorhinal cortex lesion in adult rat. Brain Res Mol Brain Res 9: 191-195, 1991.
31. Leduc V, Jasmin-Bélanger S and Poirier J: APOE and cholesterol homeostasis in Alzheimer's disease. Trends Mol Med 16: 469-477, 2010.
32. Li YL, Wu LW, Zeng LH, Zhang ZY, Wang W, Zhang C and Lin NM: ApoC1 promotes the metastasis of clear cell renal cell carcinoma via activation of STAT3. Oncogene 39: 6203-6217, 2020.
33. Zhang H, Wang Y, Liu C, Li W, Zhou F, Wang X and Zheng J: The Apolipoprotein C1 is involved in breast cancer progression via EMT and MAPK/JNK pathway. Pathol Res Pract 229: 153746, 2022.
34. Takano S, Yoshitomi H, Togawa A, Sogawa K, Shida T, Kimura F, Shimizu H, Tomonaga T, Nomura F and Miyazaki M: Apolipoprotein C-1 maintains cell survival by preventing from apoptosis in pancreatic cancer cells. Oncogene 27: 2810-2822, 2008.
35. Wang HJ, Ma YX, Wang AH, Jiang YS and Jiang XZ: Expression of apolipoprotein C1 in clear cell renal cell carcinoma: An oncogenic gene and a prognostic marker. Kaohsiung J Med Sci 37: 419-426, 2021.
36. Trougakos IP, So A, Jansen B, Gleave ME and Gonos ES: Silencing expression of the clusterin/apolipoprotein j gene in human cancer cells using small interfering RNA induces spontaneous apoptosis, reduced growth ability, and cell sensitization to genotoxic and oxidative stress. Cancer Res 64: 1834-1842, 2004.
37. Delbridge AR, Grabow S, Strasser A and Vaux DL: Thirty years of BCL-2: Translating cell death discoveries into novel cancer therapies. Nat Rev Cancer 16: 99-109, 2016.
38. Burlacu A: Regulation of apoptosis by Bcl-2 family proteins. J Cell Mol Med 7: 249-257, 2003.
39. Lowe SW and Lin AW: Apoptosis in cancer. Carcinogenesis 21: 485-495, 2000.
40. Hu W and Xiao Z: Formononetin induces apoptosis of human osteosarcoma cell line U2OS by regulating the expression of Bcl-2, Bax and MiR-375 in vitro and in vivo. Cell Physiol Biochem 37: 933-939, 2015.
41. Zhao S, Zhang Y, Lu X, Ding H, Han B, Song X, Miao H, Cui X, Wei S, Liu W, *et al*: CDC20 regulates the cell proliferation and radiosensitivity of P53 mutant HCC cells through the Bcl-2/Bax pathway. Int J Biol Sci 17: 3608-3621, 2021.
42. Huang LL, Wang Z, Cao CJ, Ke ZF, Wang F, Wang R, Luo CQ, Lu X and Wang LT: AEG-1 associates with metastasis in papillary thyroid cancer through upregulation of MMP2/9. Int J Oncol 51: 812-822, 2017.
43. Zaltsman Y, Shachnai L, Yivgi-Ohana N, Schwarz M, Maryanovich M, Houtkooper RH, Vaz FM, De Leonardis F, Fiermonte G, Palmieri F, *et al*: MTCH2/MIMP is a major facilitator of tBID recruitment to mitochondria. Nat Cell Biol 12: 553-562, 2010.
44. Grinberg M, Schwarz M, Zaltsman Y, Eini T, Niv H, Pietrokovski S and Gross A: Mitochondrial carrier homolog 2 is a target of tBID in cells signaled to die by tumor necrosis factor alpha. Mol Cell Biol 25: 4579-4590, 2005.
45. Khan DH, Mullokandov M, Wu Y, Voisin V, Gronda M, Hurren R, Wang X, MacLean N, Jeyaraju DV, Jitkova Y, *et al*: Mitochondrial carrier homolog 2 is necessary for AML survival. Blood 136: 81-92, 2020.
46. Arigoni M, Barutello G, Riccardo F, Ercole E, Cantarella D, Orso F, Conti L, Lanzardo S, Taverna D, Merighi I, *et al*: miR-135b coordinates progression of ErbB2-driven mammary carcinomas through suppression of MID1 and MTCH2. Am J Pathol 182: 2058-2070, 2013.
47. Liu L, Chai L, Ran J, Yang Y and Zhang L: BAI1 acts as a tumor suppressor in lung cancer A549 cells by inducing metabolic reprogramming via the SCD1/HMGCR module. Carcinogenesis 41: 1724-1734, 2020.
48. Wu Z, Wu J, Zhao Q, Fu S and Jin J: Emerging roles of aerobic glycolysis in breast cancer. Clin Transl Oncol 22: 631-646, 2020.
49. Li L, Ji Y, Zhang L, Cai H, Ji Z, Gu L and Yang S: Wogonin inhibits the growth of HT144 melanoma via regulating hedgehog signaling-mediated inflammation and glycolysis. Int Immunopharmacol 101: 108222, 2021.
50. Sottnik JL, Lori JC, Rose BJ and Thamm DH: Glycolysis inhibition by 2-deoxy-D-glucose reverts the metastatic phenotype in vitro and in vivo. Clin Exp Metastasis 28: 865-875, 2011.
51. Shen S, Yao T, Xu Y, Zhang D, Fan S and Ma J: CircECE1 activates energy metabolism in osteosarcoma by stabilizing c-Myc. Mol Cancer 19: 151, 2020.
52. Zhao SJ, Shen YF, Li Q, He YJ, Zhang YK, Hu LP, Jiang YQ, Xu NW, Wang YJ, Li J, *et al*: SLIT2/ROBO1 axis contributes to the Warburg effect in osteosarcoma through activation of SRC/ERK/c-MYC/PFKFB2 pathway. Cell Death Dis 9: 390, 2018.
53. Maryanovich M, Zaltsman Y, Ruggiero A, Goldman A, Shachnai L, Zaidman SL, Porat Z, Golan K, Lapidot T and Gross A: An MTCH2 pathway repressing mitochondria metabolism regulates haematopoietic stem cell fate. Nat Commun 6: 7901, 2015.